

Formulation And Evaluation Of Tetanus Toxoid-Loaded Nanostructured Lipid Particles

Kavita Rani¹, Amit Kumar J. Raval², Dinesh Kaushik³, Rajesh Khathuriya⁴

¹Research scholar, Pacific Academy of Higher Education and Research University, Udaipur, Rajasthan, India

²Associate Professor, Pacific Academy of Higher Education and Research University, Udaipur, Rajasthan, India

³Associate Professor, Hindu College of Pharmacy, Sonipat, Haryana, India

⁴Pacific College of Pharmacy, Pacific Academy of Higher Education and Research University, Udaipur, Rajasthan, India

E-mail: ¹kavitasharma.pharma@gmail.com

Abstract: Nanotechnology is regarded as the most imminent technology of 21st century and is contemplated as a big boon in the cosmetic industry. In the present investigation, non-aggregated cationic and unmodified nanoparticles (TT-C-NLPs10 and TTNLPs1) were prepared. In addition, spherical shape, crystalline architecture and cationic charge were also noticed. Furthermore, integrity and conformational stability of TT were maintained as evidenced by symmetrical position of bands and superimposed spectra, in SDS-PAGE and circular dichroism.

Keywords: Tetanus, toxoid, nanoparticles, nanotechnology.

1. INTRODUCTION

Targeted delivery of antigens to antigen-presenting cells (APCs) is a key requirement for generation of both humoral and cellular immune responses against infectious diseases, immunological disorders and cancer [1]. The magnitude of immune response is generally governed by particle size, surface charge, route of administration and hydrophobicity of particulate system. Various preparation methods for NP from biodegradable polymers are known, including emulsification/solvent evaporation and interfacial phase deposition induced by salting out or solvent displacement. The formulation of suitable colloidal antigen carriers, which must be biodegradable and biocompatible, is a difficult task [2-5].

History and development of nanomaterials

Humans already exploited the reinforcement of ceramic matrixes by including natural asbestos nanofibers more than 4,500 years ago [6].

The Ancient Egyptians were also using NMs more than 4000 years ago based on a synthetic chemical process to synthesize ≈ 5 nm diameter PbS NPs for hair dye [7].

“Egyptian blue” was the first synthetic pigment which was prepared and used by Egyptians using a sintered mixture nanometer-sized glass and quartz around 3rd century BC [8]. Egyptian blue represents a multifaceted mixture of $\text{CaCuSi}_4\text{O}_{10}$ and SiO_2 (both glass and quartz). In ancient geographical regions of the Roman Empire, including countries such as Egypt, Mesopotamia, and Greece, the extensive use of Egyptian blue for decorative purposes has been observed during archaeological explorations.

The synthesis of metallic NPs via chemical methods dates back to the 14th and 13th century BC when Egyptians and Mesopotamians started making glass using metals, which can be cited as the beginning of the metallic nanoparticle era [9].

2. MATERIAL AND METHODS

Tetanus toxoid was obtained from Panacea Biotech, New Delhi, India. All the materials used were of analytical grade.

Preparation and characterization of tetanus toxoid-loaded cationic non-aggregated nanostructured lipid particles

In the present investigation, nanostructured lipid particles (NLPs) of stearic acid were employed as an immune-adjuvant for delivery of tetanus toxoid (TT) antigen. Further, cationic lipid (DDAB18) was incorporated in the composition of NLPs to induce the cationic charge. Cationic nanoparticles have the ability to improve the transport of an antigen in to the dendritic cells and consequently the humoral and cellular immunity. Hence, TT was adsorbed on to the surface of non-aggregated NLPs (TT-NLPs1) and non-aggregated CNLPs (TT-C-NLPs 1–10) by adsorption method [10] that were constructed by solvent diffusion method [11]. Ethanol and acetone mixture was used as an organic phase to dissolve the stearic acid and DDAB18. This mixture was then poured into hot distilled water under mechanical stirring to separate the lipid nanoparticles in aqueous phase. The addition of trehalose, a cryoprotectant imparted the nonaggregation behaviour in nanoparticles by preventing the adherence phenomena [12][Table 1]

Characterisation of the formulated nanoparticles

Particle size and zeta potential

Particle size distribution and zeta-potential of nanoparticles were measured by particle size analyse. In brief, 5mg quantity of each nanoparticle sample was dispersed in 5mL of sterile normal saline (0.9% w/v NaCl) and both size distribution as well as zeta-potential was measured. The particles size and surface charge determine the cellular uptake potential of nanoparticles. The mean particle size of TT-C-NLPs10 was measured to be 50.9 ± 9.6 nm significantly (Unpaired t-test, $p < 0.05$) higher than 10.8 ± 2.4 nm of TT-NLPs1, with narrow size distribution owing to prevention of aggregation. Moreover, cationic surface charge of nanoparticles was increased as a function of the concentration of DDAB18. The zeta-potential of TT-C-NLPs10 was measured to be $+38.1 \pm 1.4$ mV significantly (Unpaired t-test, $p < 0.01$) higher than -12.4 ± 1.2 mV of TT-NLPs1. All measurements were made at 25°C in triplicate[13]

Table 1: Different formulations of nanoparticles

Compositions	Stearic acid: DDAB18	Particle size(nm)	Zeta potential(mV)
TT-NLPs1	50mg:0mg	10.8 ± 2.4	-12.4 ± 1.2
TT-C-NLPs1	50mg:50mg	44.4 ± 5.1	$+1.23 \pm 2.4$
TT-C-NLPs2	50 mg:100 mg	46.1 ± 4.3	$+8.4 \pm 3.4$
TT-C-NLPs3	50mg:150 mg	45.4 ± 3.8	$+19.2 \pm 2.4$
TT-C-NLPs4	50 mg:200 mg	46.2 ± 6.4	$+28.2 \pm 3.8$
TT-C-NLPs5	50mg:250 mg	43.4 ± 3.8	$+33.4 \pm 9.2$
TT-C-NLPs6	50 mg:300 mg	40.8 ± 1.2	$+35.2 \pm 2.3$
TT-C-NLPs7	50 mg:350 mg	56.4 ± 3.4	$+36.1 \pm 2.1$
TT-C-NLPs8	50 mg:400 mg	46.3 ± 2.1	$+36.9 \pm 2.6$

TT-C-NLPs9	50 mg:450 mg	48.6±3.2	+37.2±2.1
TT-C-NLPs10	50 mg:500 mg	50.9±9.6	+38.1±1.4

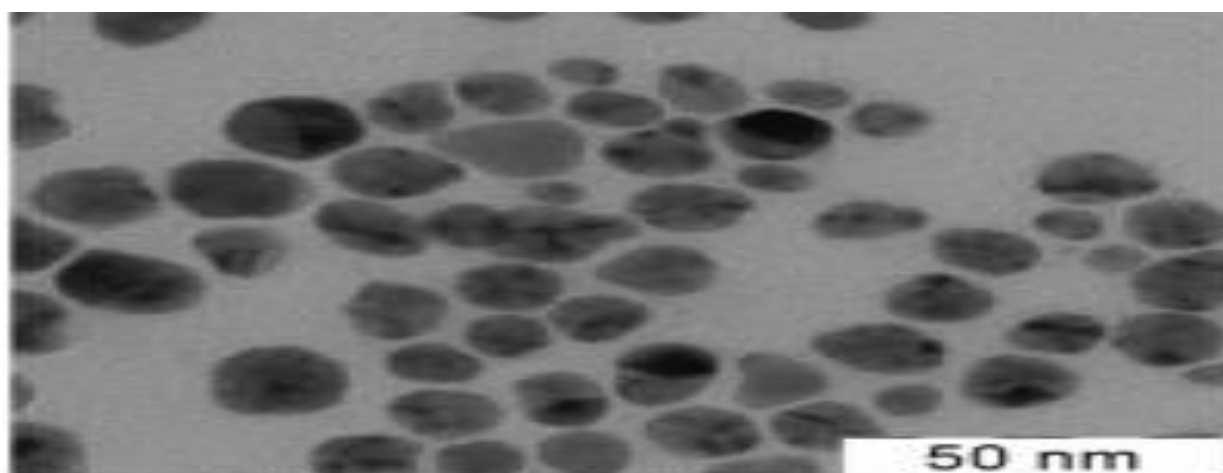


Fig 1: transmission electron microscopy (TEM) of Non-aggregated TT-C-NLPs10

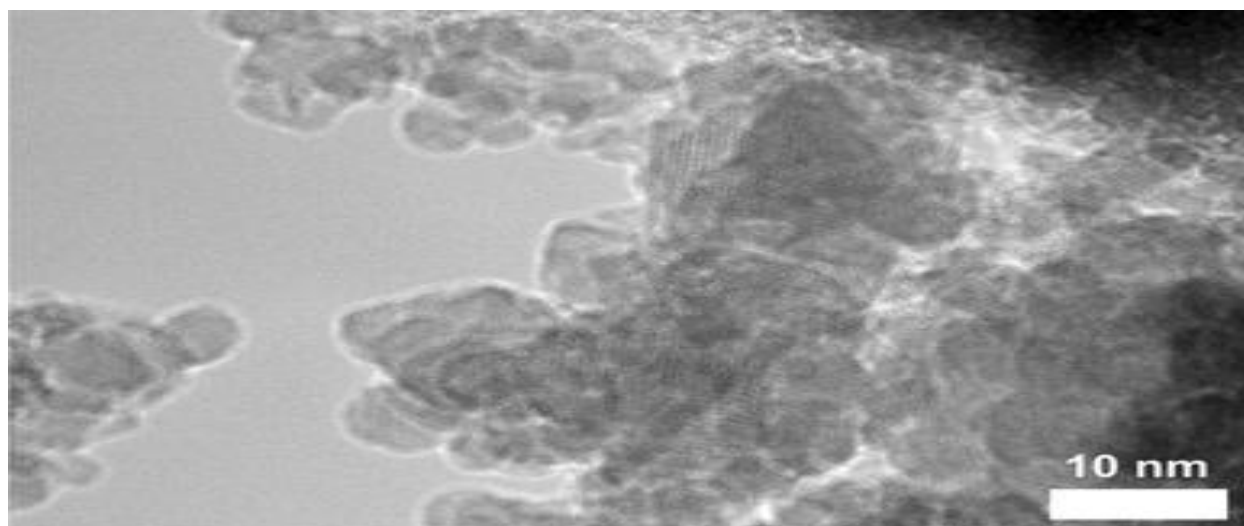


Fig 2: transmission electron microscopy (TEM) of Non-aggregated TT-NLPs1

Transmission electron microscopy (TEM)

The surface topography of nanoparticles was examined by using TEM maintained at the voltage of 80 kV. In brief, an aqueous dispersion of each sample of nanoparticles was drop cast onto a carbon coated copper grid and grid was air dried at room temperature before loading it into the microscope[14]. TEM was employed to determine the shape and surface morphology of nanoparticles. We observed that both TT-NLPs1 and TT-CNLPs 10 were smooth and spherical in shape. The particle size distribution in both samples was measured below <100 nm, consistent to the result of particle size analysis. [Fig 1,2].

Powder X-ray diffraction

The powder X-ray diffraction (PXRD) pattern was recorded using Ni filtered, CuK α radiation, voltage of 60 kV and current of 50 mA.[15] The scanning rate employed was 1°/min over the 10° to 60° diffraction angle (2 θ) range. The PXRD pattern of NLPs1 and C-NLPs10 was recorded. The crystalline architecture of nanoparticles was elucidated using PXRD technique. The PXRD pattern of NLPs1 showed diffused peaks with low intensities,

indicating the amorphous architecture. In contrast, this amorphous architecture was slightly altered upon the addition of cationic surfactant, DDAB18 in C-NLPs10 that exhibited few sharp peaks[fig3]

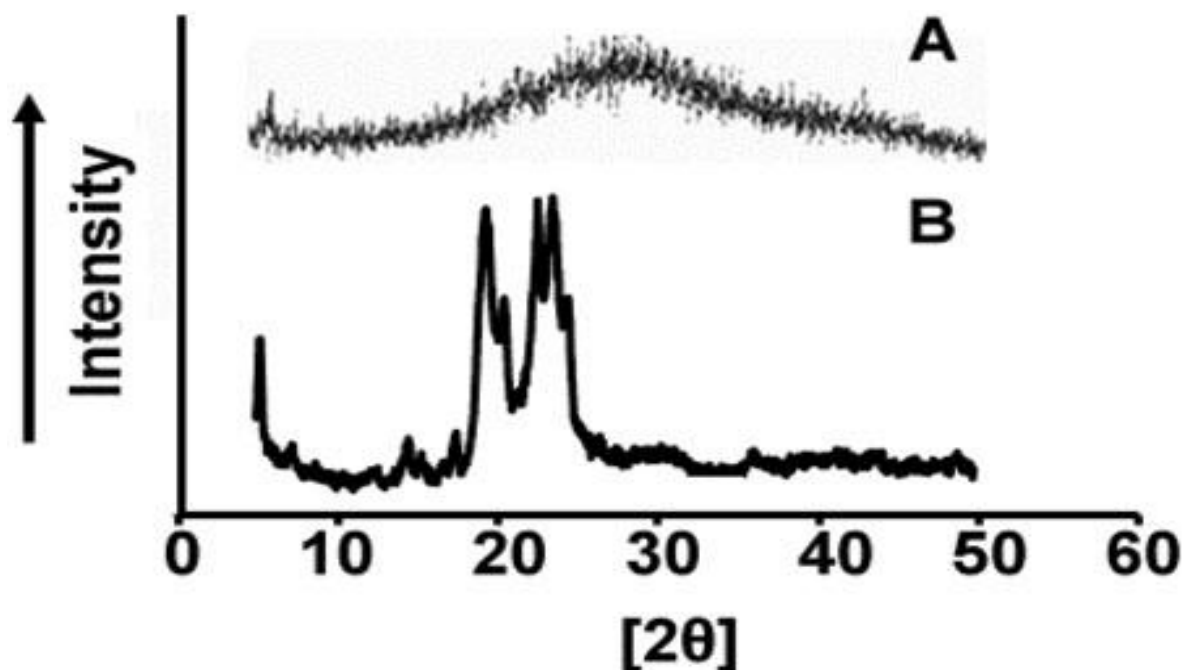


Fig 3: Powder X-ray diffraction (PXRD) pattern of (A) Non-aggregated NLPs1, and (B) Non-aggregated C-NLPs10 scanned between 10 and 60^o at 2h range. The PXRD pattern of NLPs1 exhibited diffused peaks with low intensities, indicating the amorphous geometry whilst C-NLPs10 exhibited somewhat crystalline architecture due to the presence of few sharp peaks.

Antigen-loading capacity and adsorption isotherm

The antigen-loading capacity of TT-C-NLPs10 was measured to be 350.9 ± 6.6 lg/100mg of nanoparticles, significantly (Unpaired ttest, p<0.001) higher than 55.8± 2.4 lg/100mg of TT-NLPs1 . Hence, CNLPs10 generated remarkably higher affinity for TT.[Table 2]

Table 2: Antigen-loading capacity

Compositions	Stearic acid: DDAB18	Protein loading capacity(µg/100 mg of NLPs)
TT-NLPs1	50mg:0mg	55.8±2.4
TT-C-NLPs1	50mg:50mg	92.4±5.1
TT-C-NLPs2	50 mg:100 mg	110.1±4.3
TT-C-NLPs3	50mg:150 mg	121.4±3.8
TT-C-NLPs4	50 mg:200 mg	139.9±6.4
TT-C-NLPs5	50mg:250 mg	213.4±3.8
TT-C-NLPs6	50 mg:300 mg	240.8±7.2
TT-C-NLPs7	50 mg;350 mg	256.4±3.9
TT-C-NLPs8	50 mg:400 mg	266.3±2.1
TT-C-NLPs9	50 mg:450 mg	298.6±3.2
TT-C-NLPs10	50 mg:500 mg	350.9±6.6

Gel electrophoresis

The SDS-PAGE was used to ascertain the stability and integrity of TT adsorbed on to the lipid nanoparticles[16] The structural integrity of TT isolated from TT-NLPs1 and TT CNLPs10 was compared with pure TT. The stability of TT was maintained in both TT-NLPs1 and TT-C-NLPs10, as evident by symmetrical position of bands. Moreover, the absence of additional bands in both formulations further confirmed the stability of TT throughout the adsorption process.[Fig 4]

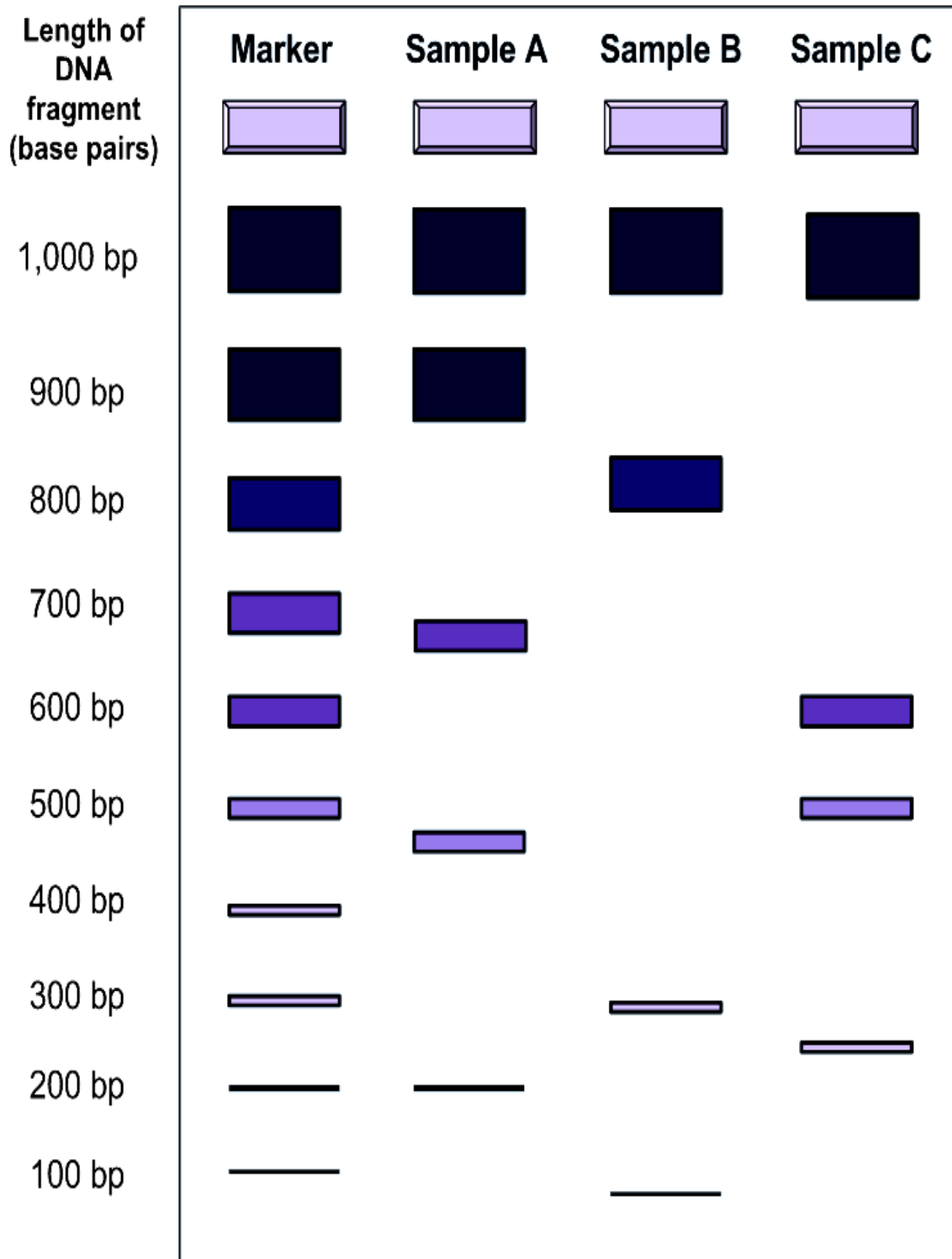


Fig 4: SDS-PAGE of TT isolated from non-aggregated TT-NLPs1, TT-C-NLPs10 and pure TT. The stability of TT was maintained in both TT-NLPs1 and TT-C-NLPs10, as evident by symmetrical position of bands.

Sample1-Marker, sample 2-pure TT, Sample 3-TT-NLPs1, Sample 4-TT-CNLPs10

Circular dichroism

The far-ultraviolet circular dichroism (CD) spectrum of pure TT (100 $\mu\text{g/mL}$) and TT (100 $\mu\text{g/mL}$) isolated from non-aggregated TT-NLPs1 and non-aggregated TT-C-NLPs4 was scanned between 190 to 300 nm at 4 $^{\circ}\text{C}$ with constant nitrogen flushing using instrument in PBS (pH 7.4) [16]. The specifications of instrument were 0.5 s scan speed; 200 nm/min sensitivity; 100 m degree and 1 nm spectra bandwidth. Three scans per sample were taken and results were expressed as residual ellipticity $[\theta]$ ($\text{deg cm}^2 \text{dmol}^{-1}$).

$[\theta] = \frac{1}{2} h \frac{1}{l} h = 10 C l \text{MRW}$

h_{abs} is measured ellipticity in degrees, C is concentration in mg/mL , l is light path length in cm and MRW is mean residual weight.

Far-UV CD is a refined approach for examination of secondary structure of antigens. Overlay CD spectra of pure TT and TT isolated from TT-NLPs1 and TT-C-NLPs10 are presented below. We observed that TT antigen was conformationally stable throughout the adsorption process as apparent by superimposed CD spectra of test samples with the CD spectrum of pure TT [fig 5]

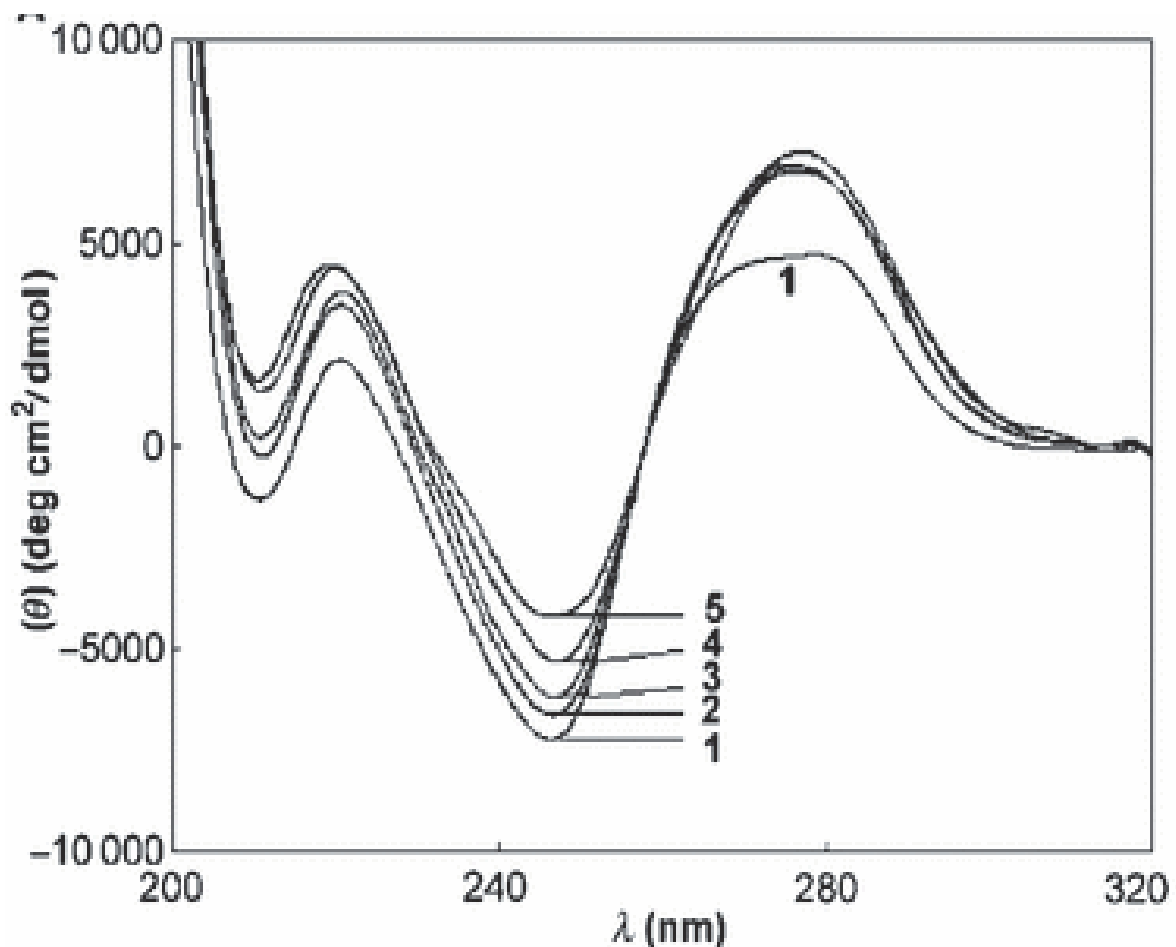


Fig 5: Circular dichroism (CD) spectrum of pure TT and TT isolated from nonaggregated TT-NLPs1 and TT-C-NLPs4,8,10 The antigen was observed to be conformationally stable

throughout the adsorption process as apparent by superimposed CD spectra of test samples with the CD spectrum of pure TT. Each experiment was carried out in triplicate (n¹/43).

3. CONCLUSION

In conclusion, we have demonstrated that tailoring non-aggregated cationic lipid nanoparticles may be an efficient immune adjuvant for antigens like TT. Particularly, cationization and induction of non-aggregation behaviour in lipid nano particles intensified the sensibility for macrophage cells and possess less diffusivity and restricted movement.

4. REFERENCES

- [1] W. Norde. Adsorption of proteins from solution at the solidliquid interface. *Adv. Colloid Interface Sci.* 1986; 25:267–340.
- [2] H. O. Alpar and A. J. Almeida. Identification of some of the physico-chemical characteristics of microspheres which influence the induction of the immune response following mucosal delivery. *Eur. J. Pharm. Biopharm.* 1994;40:198–202.
- [3] W. Norde and J. Lyklema. The adsorption of human plasma albumin and bovine pancreas ribonuclease at negatively charged polystyrene surfaces. I. Adsorption isotherms: effect of charge, ionic strength, and temperature. *J. Colloid Interface Sci.* 1978;66:257–265.
- [4] E. Nyilas, T. H. Chiu, and G. A. Herzlinger. Thermodynamics of native protein/foreign surface interactions. I. Calorimetry of the human gamma-globulin/glass system. *Trans. Am. Soc. Artif. Intern. Organs* 1974;20:480–490 .
- [5] T. H. Chiu, E. Nyilas, and D. M. Lederman. Thermodynamics of native protein/foreign surface interactions. IV. Calorimetric and microelectrophoretic study of human fibrinogen sorption onto glass and LTI-carbon. *Trans. Am. Soc. Artif. Intern. Organs* 1976;22:498–513.
- [6] Heiligtag, F. J.;Niederberger, M. Mater. Today 2013;16:262–271.
- [7] Walter, P.; Welcomme, E.; Hallégot, P.; Zaluzec, N. J.; Deeb, C.; Castaing, J.; Veysseyre, P.; Bréniaux, R.; Lévêque, J.-L.; Tsoucaris, G. *Nano Lett.* 2006; 6:2215–2219.
- [8] Johnson-McDaniel, D.;Barrett, C. A.;Sharafi, A.;Salguero, T. T. J. *Am. Ceram. Soc.* 2013;135:1677–1679.
- [9] Schaming, D.; Remita, H. *Found Chem.* 2015;17:187–205.
- [10] Susan Budavari, ed. (1989).*Merck Index* (11th ed.).Rahway, New Jersey:Merck & Co., Inc. p. 8761.ISBN978-0-911910-28-5.
- [11] Erni C, Suard C, Freitas S, Dreher D, Merkle HP, Walter E. Evaluation of cationic solid lipid microparticles as synthetic carriers for the targeted delivery of macromolecules to phagocytic antigen-presenting cells. *Biomaterials*, 2002;23:4667–76.
- [12] Oyewumi MO, Kumar A, Cui Z. Nano-microparticles as immune adjuvants: Correlating particle sizes and the resultant immune responses. *Expert Rev Vaccines*, 2010;9:1095–107.
- [13] Almeida AJ, Souto E. Solid lipid nanoparticles as a drug delivery system for peptides and proteins. *Adv Drug Deliv Rev*, 2007;59:478–90.
- [14] Wang Z, Zhu K, Bai W, Jia B, Hu H, Zhou D, Zhang X, Zhang X,Xie Y, Bourguine MM, et al. Adenoviral delivery of recombinant hepatitis B virus expressing foreign antigenic epitopes for immunotherapy of persistent viral infection. *J Virol*,2014;88:3004–15.

- [15] Almeida AJ, Souto E. Solid lipid nanoparticles as a drug delivery system for peptides and proteins. *Adv Drug Deliv Rev*,2007;59:478–90.
- [16] Hu FQ, Jiang SP, Du YZ, Yuan H, Ye YQ, Zeng S. Preparation and characterization of stearic acid nanostructured lipid carriers by solvent diffusion method in an aqueous system. *Colloids Surf B Biointerfaces*, 2005;45:167–73.